Table 2 Inviscid two-shock-theory model conditions

Station	Free-stream	Ramp	Combustor
p, psia	0.12	4.8	27.3
T, °K	88	647	1160
M	11.0	3.5	2.1
U, fps	6800	5800	4600

III. Summary of Results

Tests without fuel injection

Considerable effort[3] was expended before an acceptable flow was obtained in the two-dimensional combustor. The primary source of difficulty was the interaction of the shock wave from the cowl lip with the inlet boundary layer and the Prandtl-Meyer expansion at the intersection of the inlet and combustor. This problem was compounded by significant source flow effects which caused a decay in static pressure along the inlet ramp surface and the finite ramp width (3 in.) which caused cross flows in the ramp boundary layer and was a possible cause of the early boundary-layer transition. Experimental heat-transfer rates to the ramp indicated that the end of transition from a laminar to a turbulent boundary layer occurred at approximately 3 in. from the plate leading edge, whereas the estimated length for the end of transition (using current transition literature) was approximately 6–7 in.

The measured average static pressure in the combustor was ≈13.5 psia and the average static temperature and Mach number inferred from measured values of static and Pitot pressures at the combustor exit were 1200°K and 1.9 respectively. Inviscid two-shock theory estimates are given in Table 2. Approximately 50% of the estimated pressure was obtained. Repeatable, steady operation of the model was obtained when a porous ramp was used to bleed off part of the inlet boundary layer and the cowl lip, positioned so that the second shock impinged as close as possible to the intersection of the ramp and combustor.

Tests with fuel injection

Hydrogen fuel, at 300°K total temperature, was injected from either sonic orifices in the upper combustor plate—normal injection—or sonic orifices in the struts (see Fig. 1). With a cold driver gas temperature (300°K), satisfactory combustion[4] was demonstrated with strut injection only, as shown in Figs. 3 and 4.

The driver gas was heated to 480°K which increased the total temperature and pressure as shown in Table 1. The combustor static pressure level increased from 13.5 to 18.2 psia and the static temperature increased from 1200° to 1530°K. The average Mach number at the combustor exit did not change significantly from the previous value of ≈1.9.

Hydrogen fuel at 300°K was again injected with satisfactory combustion[4] data obtained for strut injection tests only as shown in Figs. 5 and 6. The sodium-line-reversal measurements confirmed significant increases in static temperature due to combustion on strut injection tests only.

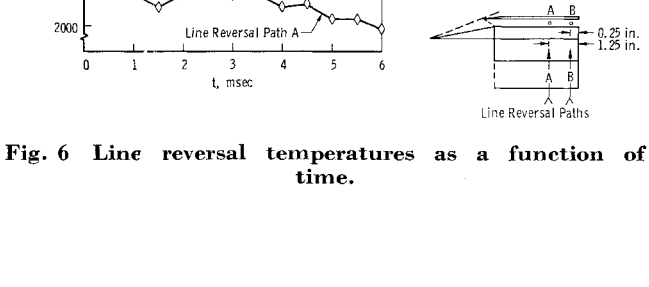

Fig. 6 Line reversal temperatures as a function of time.

IV. Conclusions

It has been demonstrated that it is possible to carry out supersonic combustion tests for development of instrumentation and analytical techniques applicable to SCRAMjets within a useful test time of approximately 3 msec in a shock tunnel.

References

[1] Griffith, B. J. and Weddington, E. D., "Recent Refinements and Advancements of Hypersonic Testing Techniques in the 108-inch Tunnel F of the von Kármán Gas Dynamics Facility," *Proceedings of the Fourth Hypervelocity Techniques Symposium*, Nov. 15–16, 1965, Arnold Engineering Development Center, Tullahoma, Tenn.

[2] Haun, J. H. and Ball, H. W., "Calibration of the Shock Tunnel Component of Counterflow Range "I" at Mach 7.5," TR-66-64 (AD 632816), May 1966, Arnold Engineering Development Center.

[3] Osgerby, I. T., Smithson, H. K., and Wagner, D. A., "Development of a Double-Oblique-Shock SCRAMjet Model in a Shock Tunnel," TR-69-59, Aug. 1969, Arnold Engineering Development Center.

[4] Osgerby, I. T., Smithson, H. K., and Wagner, D. A., "Supersonic Combustion Tests with a Double-Oblique-Shock SCRAMjet in a Shock Tunnel," TR-69-162, Feb. 1970, Arnold Engineering Development Center.

Flight Results Showing the Effect of Mass Addition on Base Pressure

J. M. Cassanto* and T. L. Hoyt†
General Electric Company, King of Prussia, Pa.

Nomenclature

P_b	= base pressure
P_∞	= freestream pressure
P_b/P_∞	= base pressure ratio
Re_L	= freestream Reynolds number based on axial length
r	= radius at any point on the base
R	= maximum base radius
M_∞	= freestream Mach number
$\dot{m}/\rho AV$	= mass addition parameter
$K_{\dot{m}}$	= ratio of base pressure with mass addition to base pressure with zero mass addition
$\Delta\theta$	= flow turning angle
ρ	= freestream density
A	= base area
V	= freestream velocity
L_{Neck}	= distance from R/V base to wake neck
R/V	= re-entry vehicle

I. Introduction

RECENT full scale re-entry flight test base pressure data in turbulent flow have shown a dependency on the heat shield material. The heat shield material, of course, determines the amount of mass addition to the boundary layer due to the ablation process. This present Note has a threefold purpose: 1) to present the flight test base pressure data results; 2) to propose a flow hypothesis mechanism which explains how mass addition affects base pressure; and, 3) to show correlations of the base pressure ratio data with mass addition rate.

Presented as Paper 70-109 at the AIAA 8th Aerospace Sciences Meeting, New York, January 19–21, 1970; submitted February 9, 1970; revision received May 25, 1970. This work was performed under Air Force Contract AF 04(694)914.

* Supervising Engineer, Aerodynamics Laboratory, Re-entry and Environmental Systems Division. Member AIAA.

† Engineer, Aerodynamics Laboratory, Re-entry and Environmental Systems Division. Associate Member AIAA.

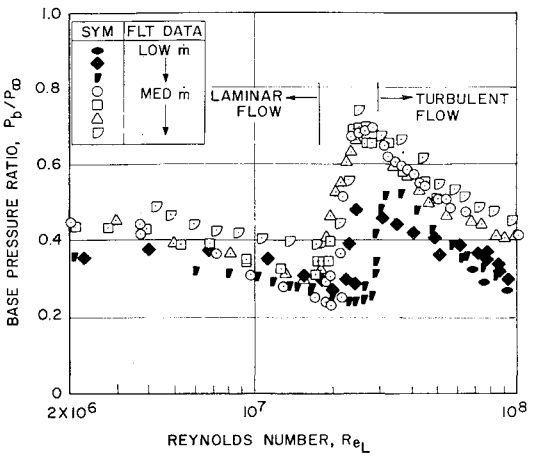

Fig. 1 Flight results: base pressure ratio data vs Reynolds number.

II. *R/V* Flight Configuration, Entry Conditions, and Instrumentation

The *R/V* flight configurations were nearly identical slender cones having full dome afterbodies. Re-entry conditions and trajectories were essentially identical for all flights, and the angle of attack was nominally zero during the period

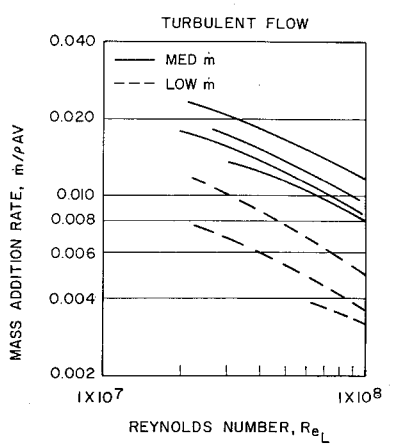

Fig. 2 Calculated mass addition rate vs Reynolds number.

when the data were obtained. The Mach number during re-entry for the data presented was hypersonic and varied between $M_\infty \sim$ 20–22. Two basic heat shield materials were utilized during the flight test series. The heat shield materials flown fall into two broad categories: medium

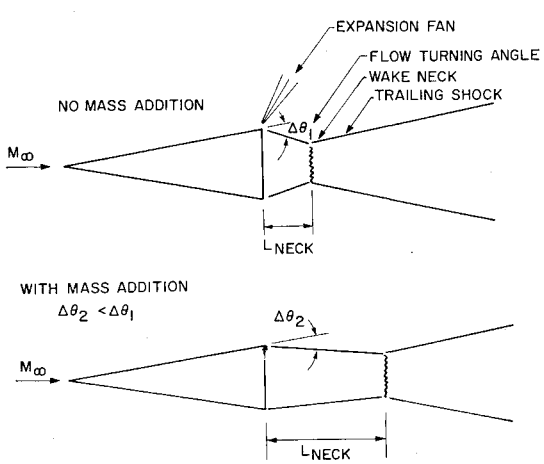

Fig. 3 Flow geometry for turbulent flow with and without mass addition.

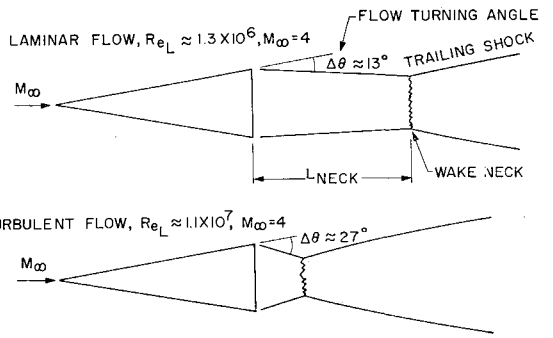

Fig. 4 Flow geometry for nonablator in laminar and turbulent flow.

ablators (having average $\dot{m}/\rho AV \approx 0.014$), and light ablators (having average $\dot{m}/\rho AV \approx 0.007$) in turbulent flow.

The flight vehicles had only a single pressure port on the base located at 50% ($r/R = 0.5$) of the base radius, and 30° off center. This port was "T" tapped to a low-range (0–0.1 psia) and a high-range (0–1.0 psia) pressure transducer to obtain both laminar and turbulent data. Flight data were reduced only for that portion of the trajectory where the pressure sensors exceeded 10% of full scale to insure data validity. The data were nondimensionalized with the free-stream pressure derived from the measured atmosphere (obtained from radiosonde data) in conjunction with a radar tracking trajectory.

III. Results

The flight test base pressure ratio results plotted as a function of freestream Reynolds number are shown in Fig. 1. Data trends are mixed for the laminar flow region ($Re_L \leqslant 1.8 \times 10^7$). However, for turbulent flow ($Re_L \geqslant 3 \times 10^7$) the data are well ordered, and fall into two bands. The medium ablator flights consistently have higher base pressures (approximately 40%) than the low ablator flights as evidenced by the comparison of the open symbols with the closed symbols. The Mach number during this data taking period is essentially constant and the apparent base pressure variation with Reynolds number from 3×10^7 to 1×10^8 is in reality a mass addition effect. This is because it has been shown by controlled ground tests[1,2] that base pressure is relatively constant with Reynolds number once a turbulent boundary layer has been obtained. In addition, the $\dot{m}/\rho AV$ is decreasing in the region where the flight data were obtained. This can be seen in Fig. 2, which shows the calculated mass addition rates for each flight. The mass addition rates fall into two broad bands: medium rates $\dot{m}/\rho AV \approx 0.014$

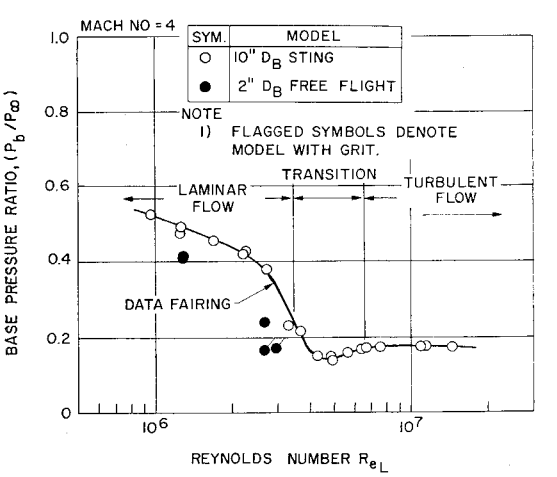

Fig. 5 Ground test base pressure data on sharp cone.

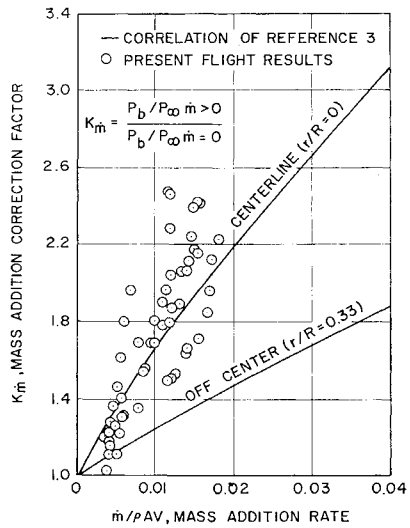

Fig. 6 Mass addition correlation.

corresponding with the flights having high base pressures and low rates $\dot{m}/\rho AV \approx 0.007$ corresponding with flights having low base pressures.

IV. Flow Mechanism Hypothesis

The following hypothesis[3,4] is postulated as the primary mechanism which accounts for the increase in base pressure with increasing mass addition. Mass addition tends to thicken the boundary layer and especially the laminar sublayer. The large laminar sublayer can result in a pseudo-laminar base flow region. The thicker boundary layer, which includes the mass flow from the ablating process, is swept into the wake region and tends to enlarge the neck of the wake and force it downstream, thus changing (decreasing) the wake expansion angle, as shown in Fig. 3. The smaller expansion angle is similar to what would be expected in laminar flow, and results in a higher base pressure ratio. This phenomena is illustrated in Figs. 4 and 5 and is based on the results of ground tests on a nonablating body.[2] The flow turning angle ($\Delta\theta$) can be seen to be less in laminar flow than turbulent flow (Fig. 4), whereas the base pressure is higher in laminar flow than turbulent flow (Fig. 5).

V. Base Pressure Mass Addition Correlation

The flight data from the seven flights correlated nicely when the ratio of base pressure with mass addition to base pressure with zero mass addition was plotted as a function of $\dot{m}/\rho AV$ (Fig. 6). Since all of the flights considered had ablative heat shields, the zero mass addition base pressure levels were obtained from the prediction technique of Ref. 3 for $\dot{m}/\rho AV = 0$. The pressure data are in qualitative agreement with the empirical correlation of Ref. 3 and show that base pressure ratio has a near linear type relationship with mass addition rate. This trend of increasing base pressure with increasing mass addition rate has also been observed in the ground test data of Refs. 5 and 6. The correlation of Ref. 3 indicates that a radial pressure gradient is present on the base due to mass addition effects. The present data were not sufficient to verify this trend. It is suspected but not verified that the correlation of the present data is unique to the mass addition distribution for these flight vehicles. Flight vehicles having different mass addition distributions (but the same approximate rates $\dot{m}/\rho AV \approx 0.007$ to 0.014) would have differences in the local conditions preceding the base. This may explain why the present data are in qualitative rather than quantative agreement with the correlation of Ref. 3.

References

[1] Whitfield, J. D. and Potter, J. L., "On Base Pressures at High Reynolds Numbers at Hypersonic Mach Numbers," TN-60-61, March 1960, Arnold Engineering Development Center, Tullahoma, Tenn.

[2] Cassanto, J. M., "Base Pressure Measurements on Free-flight and Sting Supported Modes at $M = 4$," *AIAA Journal*, Vol. 6, No. 7, July 1968, pp. 1411–1414.

[3] Cassanto, J. M. and Storer, E. M., "A Revised Technique for Predicting the Base Pressure of Sphere Cone Configurations in Turbulent Flow Including Mass Addition Effects," Aerodynamic Fundamentals Memo ALFM 68-41, Oct. 1968, General Electric Co.

[4] Cassanto J. M. and Mendelson, R. S., "Local Flow Effects on Base Pressure," *AIAA Journal*, Vol. 6, No. 6, June 1968, pp. 1182–1185.

[5] Fox, J., Zakkay, V., and Sinah, R., "A Review of Some Problems in Turbulent Mixing," Rept. NYU-AA-66-63, Sept. 1966, New York Univ.

[6] Lewis, J. E. and Chapkis, R. L., "Mean Properties of the Turbulent Near Wake of a Slender Body With or Without Base Injection," *AIAA Journal*, Vol. 7, No. 5, May 1969, pp. 835–841.

Mean Density and Temperature Data in Wakes of Hypersonic Spheres

J. G. G. Dionne* and L. Tardif*
Defence Research Establishment Valcartier, Quebec, Canada

THE successful use of electron beam fluorescence probes in the study of mass density and temperature in shock tubes and shock tunnels[1–3] has led experimenters to use this probing system to study wakes of hypersonic projectiles.[4,5] The superiority of such a system is essentially its minimum interference with the gas flow, and its most serious drawback is its limited effectiveness at ambient pressures above 10 torr.

The electron beam generator itself and the optical system used to measure the induced fluorescence have been detailed elsewhere[5]; the main characteristics are a 2 milliamperes beam capability at 100 KV for the generator and a large-aperture optical system. The field of view is defined geometrically by a slit, and spectrally by an interference filter. The bulk of emission induced by the electrons in nitrogen or air is represented by the N_2 second positive and by the N_2 first negative systems[6]; for both intensity and linearity reasons, the latter is preferred at pressures below one torr, and the former, at pressures above three torr. Muntz[1] has studied the excitation and emission processes for the first negative system, and Camac[7] has reported that the emission of the second positive system is produced not by the primary electrons but by the secondary electrons formed by the primary beam. The emission will thus be produced around the primary beam within the range of the secondary electrons. As the pressure increases, the effective range of the secondary electrons decreases, while the primary beam spreads out. Measurements have shown that the primary beam spreading increases rapidly with the pressure-distance product. Also, the effective beam width is larger at 3371 Å $N_2[2P(0,0)]$ than at 3914 Å $N_2^+[1N(0,0)]$, particularly at pressures below one torr, as the secondary electron range increases with decreasing pressure while a negligible beam spreading of the primary beam is experienced.

Received February 9, 1970; revision received May 15, 1970. The authors are indebted to members of the Defence Research Establishment Valcartier (DREV), Aerophysics Division, for their support. The work is part of a joint DREV-Advanced Research Projects Agency (ARPA) program for investigation of the hypersonic turbulent wake under ARPA Order 133.

* Defense Scientific Service Officer.